Available online at www.sciencedirect.com

ScienceDirect

Resource-Efficient Technologies 3 (2017) 101–112

www.elsevier.com/locate/reffit

A study of CO_2 flooding on wave velocities in the Naharkatiya oil reservoir of Upper Assam Basin

Subrata Borgohain Gogoi *, Miranda Kakoty

Department of Petroleum Technology, Dibrugarh University, Dibrugarh, Assam, India

Received 20 June 2016; accepted 30 December 2016

Available online 6 March 2017

Abstract

This paper studies the compressional-wave and shear-wave velocities in the laboratory in six conventional core plugs. These plugs were obtained from a depth of more than 3000 m from the producing horizons of Naharkatiya oil reservoir of Upper Assam Basin, India. The porosities of the conventional core plugs were from 9.67 to 25.8% and that of unconsolidated sand pack was 47%. These plugs and sand pack were saturated with *n*-hexadecane before CO_2 flooding. It was observed that during flooding compressional-wave velocities decreased more than the shear wave velocities. These decreases in wave velocity depend on confining pressure, pore pressure, porosity and temperature of the plugs. Increasing pore pressure at constant confining pressure not only keeps the pores and cracks open but also reduces the confining pressure effect and increases the CO_2 density. Higher pore pressures causes larger decrease in both compressional and shear wave velocities. In case of conventional core plugs which are consolidated, having lower porosities tends to decrease the CO_2 effect. In unconsolidated sand pack the flooding effect is large even though porosity is high because the bulk modulus of the sand is low. The experimental and the theoretical analyses in this paper show that the decrease in compressional-wave velocities caused by CO_2 flooding makes it possible to track CO_2 front movements and monitor CO_2 flooding process in the reservoir.

Keywords: Compressional-wave velocity; Shear-wave velocity

1. Introduction

The oil recoveries at the end of primary and secondary recovery processes are generally in the range of 20–40% of the original oil in place (OOIP) [1]. Work on chemical EOR specially surfactant flooding, alkali surfactant polymer flooding, micellar alkali polymer flooding showed enhance oil recovery [1–9]. However, these methods carry with them their own inherent risks in addition to the economic costs; the chemical pathways through which these products are generated often use toxic chemicals, such as ethylene oxide in the production of nonionic surfactants [10–12]. Additionally, the products themselves may be damaging to the environment, especially when present with crude oil [13,14]. Such risks have directed attention towards finding environmentally-friendly and economically feasible alternatives. Therefore the need of the hour is to develop eco-friendly and economical Enhanced Oil Recovery (EOR) processes which can recover the 80–60% of the OOIP left after primary and secondary recovery processes. CO_2-EOR and sequestration presents an opportunity for us to address climate change concerns while still enjoying the benefits of recovering more of the fossil fuels by way of EOR. However, there are several challenges that must be met. Gogoi [15] dealt with the injection of CO_2 for the purpose of EOR in mature and depleted oil and gas reservoirs of Upper Assam Basin, India. Of course not all reservoirs of Upper Assam Basin are suitable for CO_2 flooding, but considerable effort is currently being made in research laboratories and oil industries to implement large scale CO_2 injection projects for EOR.

With the development of better EOR methods pertaining to CO_2 flooding worldwide [16–22], methods of monitoring EOR processes are also becoming important because monitoring will help us to control the recovery processes. Seismic methods are

* Corresponding author. Department of Petroleum Technology, Dibrugarh University, Dibrugarh 786004, India. Tel.: +91 97902 99447; fax: +91 373 2370323.

E-mail addresses: subrata@dibru.ac.in; sbg6dupt@gmail.com (S.B. Gogoi).

http://dx.doi.org/10.1016/j.reffit.2016.12.011

Nomenclature

G	shear moduli, N/m^2
K	bulk moduli of the fluid saturated rock, N/m^2
K_d	bulk moduli of the dry rock, N/m^2
K_f	bulk moduli of the pore fluid, N/m^2
K_s	bulk moduli of the solid framework of the rock, N/m^2
φ	porosity, fraction
ρ	density of the material, kg/m^3
v_c	compressional velocity, m/s
v_s	shear velocity, m/s
Δt	difference in temperature, °C
μ	viscosity, cp

Notations

CO_2	carbon dioxide
$C_{16}H_{34}$	*n*-hexadecane
L	length of core plug at STP
OOIP	original oil in place
P_c	confining pressure
P_e	effective pressure
P_p	pore pressure
STP	standard temperature and pressure
Δt	travel time of compressional and shear waves
v	velocity

becoming increasingly popular for mapping of subsurface CO_2 movement during EOR or geologic sequestration [23]. Seismic methods are the most promising monitoring method; moreover, the acquisition and processing of field data by this method is also economical [24]. Seismic method in monitoring EOR process depends on velocity and amplitude change of the seismic waves. Seismic monitoring does not require shutting in of wells, so it does not disturb reservoir fluid flow because seismic waves usually cause very small strains in reservoir rocks and does not cause precipitation or adsorption of chemicals in the reservoir [25].

Injected CO_2 increases the compressibility and increases or decreases the density of the reservoir rocks, depending upon the pore pressure [17,26]. These changes will in turn effect the propagation of the seismic waves. The quantitative effect of CO_2 flooding on wave characters is not yet known; however, no laboratory or field work on such effects has not been published for any of the oil fields of India. Application of the CO_2-EOR process in the Upper Assam Basin is preferred because of the availability of CO_2 in adequate quantities from both natural and industrial sources.

The compressional and shear wave velocities were measured before and after CO_2 flooding by ultrasonic-pulse-transmission technique in six conventional core plugs obtained from the producing horizons from different wells of the same field. The conventional plugs were from the consolidated sandstone reservoir of Upper Assam Basin obtained from a depth of more than 3000 m (corresponding depths of 6 core plugs are provided in Table 1). The porosities of the plugs were from 9.67% to 25.8% and the porosity of the unconsolidated sand pack was 47%. It was found that the compressional wave velocities (v_c) were decreased greatly by CO_2 flooding especially when the pore pressures were high, while the shear wave velocities (v_s) were less affected by CO_2 flooding. From the experimental and theoretical studies it was observed that there is a decrease in v_c in hydrocarbon ($C_{16}H_{34}$) saturated rocks during CO_2 flooding. An attempt is made to calculate the velocities according to Gassmann's formula and the results were compared with experimental values. This research is expected to be useful in mapping and locating CO_2 zones, tracking CO_2 front movement and monitoring CO_2 flooding process.

Table 1
Specifications of the core plugs.

Sl. No.	Core plug	Depth (m)	Porosity (%)	Composition
1	N1	3116.03	9.67	Mainly quartz
2	N2	3114.89	12.8	Mainly quartz
3	N3	3113.76	18.6	Mainly quartz
4	N4	3210.98	21.3	Mainly quartz
5	N5	3210.12	25.8	Quartz and 23% feldspar
6	LWP sand		47	Quartz grains

2. Materials and methods

2.1. Materials

Conventional rock samples obtained from different consolidated oil producing wells were obtained from a depth of more than 3000 m from Naharkatiya oil field of Upper Assam Basin (India) producing since 1953 and is today in the late stage of depletion. The rock samples were cut into core plugs of 3.81 cm (1.5 inch) diameter and 8.9 cm (3.5 inch) length. The porosities of the plugs measured by Helium Porosimeter, model no. TPI-219 and made by Coretest Systems, were found to be in the range of 9.67–25.8% (Table 1). The unconsolidated sand pack was the Light Weight Proppant (LWP) sand from Texas (USA). A saturated hydrocarbon *n*-hexadecane ($C_{16}H_{34}$), with a straight chain molecular structure, was purchased from Merck Chemical India, Mumbai (India). At room temperature its molecular weight is 226.16 g/mol, melting point is 18 °C, boiling point is 287 °C, density at 20 °C is 0.773 g/cm^3 and viscosity at 20 °C is 3.51 cp as determined by Canon Fenski viscometer. $C_{16}H_{34}$ was used instead of crude oil as crude oil caused problems when used in the laboratory core flood apparatus. CO_2 was obtained with a tank pressure of 5.5 MPa (56 kg/cm^2) and a purity of 99.9% as purchased from Asiatic Traders, Dibrugarh, Assam, India.

2.2. Methods

The core plugs one at a time were subjected to cleaning by Soxhlet apparatus with 1:1 ratio of toluene and methanol for 48 hours and in Ultrasonic cleaner for 9 minutes and dried in the

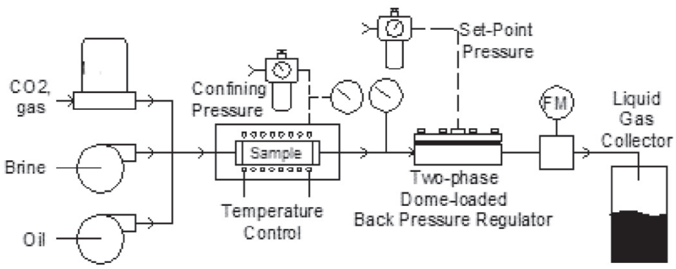

Fig. 1. Schematic diagram of the core flood apparatus, in line with Section 2.2.

Humidity Control Oven until a constant weight is maintained. Each core plug under test was fitted to the hassler core holder of the core flood apparatus (Fig. 1) and was subjected to a confining pressure (P_c) up to 22 MPa to eliminate pressure hysteresis of the velocities. v_c and v_s are determined for a sample by the transit time of ultrasonic pulses (approximately 200 kHz to 2 MHz) vs. P_c from 0 to 22 MPa in core plugs and LWP sand pack. The jacketed sample was placed either in a pressure vessel so that stresses can be applied. Temperature and pore fluid pressure were also controlled. Details of the techniques are found in Refs. [27,28]. An error analysis of the ultrasonic measurements showed that the measured ultrasonic velocities have an error smaller than 1% [29]. The same core plugs were then saturated with degassed $C_{16}H_{34}$. v_c were measured at different temperatures (30 °C, 40 °C, 60 °C and 80 °C) vs. effective pressure (P_e). v_c and v_s were measured in $C_{16}H_{34}$ saturated core plugs vs. pore pressure (P_p) with the P_c kept constant at 22 MPa. The plugs were then flooded with CO_2 at 7 MPa through one of the two pressure tubings (Fig. 2). 7 MPa is selected because if the temperature and pressure of CO_2 are both increased from standard temperature and pressure (STP) or above the critical point (31.1 °C, 7.39 MPa) it can adopt properties midway between a gas and a liquid. More specifically, it behaves as a supercritical fluid above its critical temperature and critical pressure, expanding to fill its container like a gas but its density (ρ) increases as pressure increases (Fig. 3) [15]. A valve on the pressure tubing connected to the other end of the plug was regulated to let displaced $C_{16}H_{34}$ out. After flooding by CO_2 P_p was increased to 16 MPa by injecting more CO_2. The travel time of the pulse through the sample was measured as a function of decreasing P_p. It was calculated that 50–60 vol% of $C_{16}H_{34}$ was recovered by CO_2 flooding. The temperature was controlled by a built in electric heater inside the pressure vessel and measured by a digital thermometer through a thermocouple (Fig. 1). The travel time of the electric wave through the sample was measured with a digital oscilloscope. v_c and v_s were calculated by $v = L/\Delta t$, where v = velocity (v_c or v_s); Δt = travel time of compressional and shear waves; L = core plug length at STP. MATLAB was used to perform all statistical analyses [30–32].

3. Results and discussion

Figs. 4–12 report on the velocity response of the sandstone cores with change in temperature, P_e or P_P and porosity (φ). The observed results showed the possibility of using seismic methods in mapping CO_2 zones, tracking CO_2 flood front movements and monitoring CO_2 processes in reservoir subject to CO_2-EOR.

P_e or ($P_e = P_c - P_p$) strongly effect v_c and v_s [33]. In Fig. 4 it is seen that as temperature increases v_c decreases at constant P_c similar to the case observed in Boise sandstone measured as a functions of temperature [34,35]. In the experiments P_c was kept constant with varying P_p on core plugs and found that v_c was strictly a function of both P_e and temperature t in the cores [36,37]. Above the critical temperature of CO_2, the v_c and v_s were a weak function of pressure (Fig. 5). In contrast below critical temperature, the v abruptly increases at around 6 to

Dry plugs subjected to P_c of 22 MPa

↓

In dry cores v_c & v_s versus P_p measured from 0-22 MPa

↓

Dry plugs saturated with degassed $C_{16}H_{34}$.

↓

v_c were measured in saturated $C_{16}H_{34}$ plugs at diff temps (30°C, 40°C, 60°C and 80°C) versus P_e

↓

In sat. cores v_c & v_s versus P_p [P_c = 22 MPa] were measured

↓

Saturated cores flooded with CO_2 at 7 MPa .

↓

P_p increased to 16 MPa by injecting more CO_2

Fig. 2. Experimental procedure.

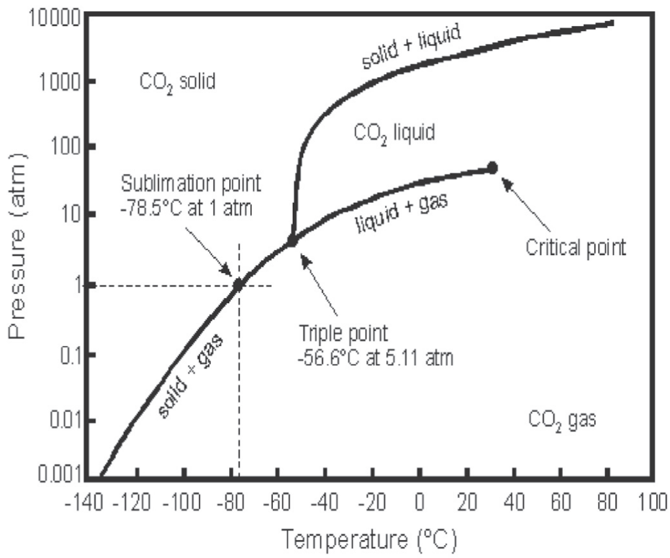

Fig. 3. Pressure–temperature phase diagram for CO_2.

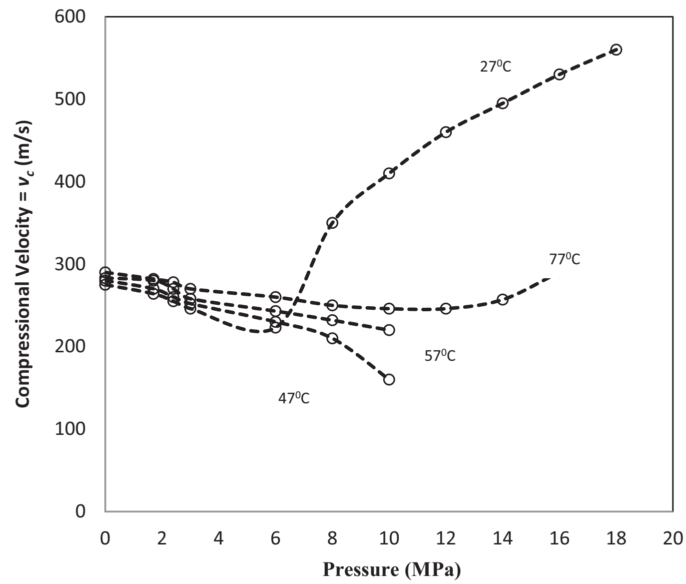

Fig. 5. v_c in CO_2 as a function of temperature and pressure.

7 MPa, because CO_2 behaves as a liquid (Fig. 3) [38]. With CO_2 in the liquid phase, the v is a strong function of P_e, increasing very fast as P_e increases (Fig. 5) which also resembles the behaviour as shown in Fig. 4. However, the v in liquid CO_2, was still much lower than that in $C_{16}H_{34}$ (Fig. 5). Unfortunately we did not measure v_s as a function of P_e in $C_{16}H_{34}$ and CO_2 saturated core plugs at different temperatures because it showed the same conclusion as in the literature [39].

As seen in column 8 of Table 2, v_c increases upon hydrocarbon saturation, which is unexpected according to Biot theory [40,41], which predicts that v_c in porous media should slightly decrease upon liquid saturation owing to increased overall density.

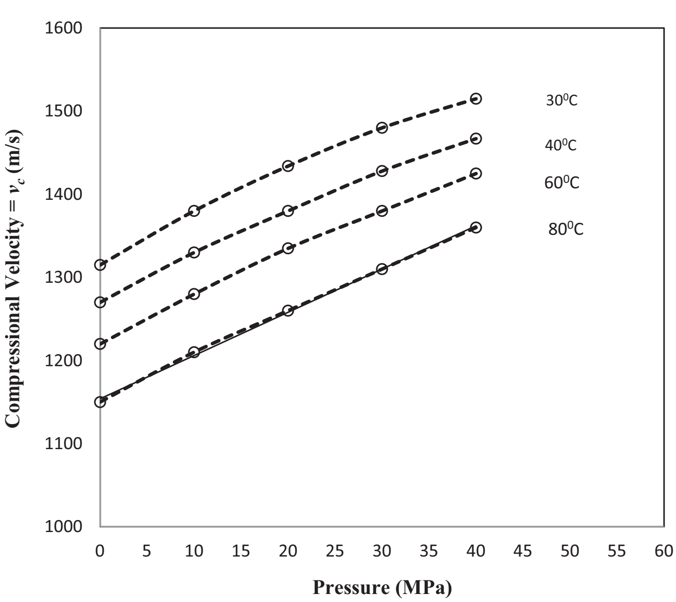

Fig. 4. v_c in n-$C_{16}H_{34}$ as a function of temperature and pressure.

In Figs. 6a, b, 7a, 8a, 9a, 10a and b it was observed that v_c and v_s decrease with the introduction of CO_2 especially at higher P_P were still high. The injected CO_2 at a temperature of 60 °C is at vapour phase, so there is no abrupt change in v_c with variation in P_P. The rock saturated with CO_2 in vapour phase shows nearly the same behaviour as dry core plugs.

At higher P_p, v_c in the CO_2 flooded cores were much lower than that in $C_{16}H_{34}$ saturated cores. These lowered v_c and v_s are apparently caused by the presence of CO_2 in the pores of the core sample.

v_c and v_s increase with increasing P_e ($P_e = P_c - P_p$) due to the closure of the microcracks of the core plugs. P_e increases when P_p decreases provided P_c is a constant like in this case P_c is 22 MPa throughout the experiments. In sedimentary rocks, the velocities tend to asymptotic values at high P_e [42].

All the v_s curves cluster in Figs. 7b, 8b and 9b which means that CO_2 basically does not affect v_s in these core plugs. However temperature has a systematic, although small effect on v_s, it was observed that at lower P_p, v_s in the CO_2 flooded cores were lower than in $C_{16}H_{34}$ saturated core plugs at the same temperature and the opposite is true at higher P_p (lower P_e).

Both Fig. 10a N5 core plug and Fig. 11 LWP sand pack have higher φ. The $C_{16}H_{34}$ saturation effect on v_c was relatively small. The $C_{16}H_{34}$ saturation increased v_p in core plugs and sand pack and this increase becomes smaller as P_p decreased. The v_s were almost the same in $C_{16}H_{34}$ saturated and CO_2 flooded samples. In other core plugs (Figs. 6a, b, 7a, b, 8a, b, 9a, b) CO_2 flooding decreased v_c. Also P_p dependence on v_p was enhanced by flooding (Fig. 10a), while v_s behaves similar to N2 (Fig. 7b), N3 (Fig. 8b), N4 (Fig. 9b) and the difference between the v_s in $C_{16}H_{34}$ saturation and CO_2 flooded N6 core plug (Fig. 10b) was small.

Since the LWP sand has very high porosity of 47%, with $C_{16}H_{34}$ saturation the increase in v_c was much lower with the decrease in P_p (Fig. 11). The CO_2 flooding effect in N6 (Fig. 10a

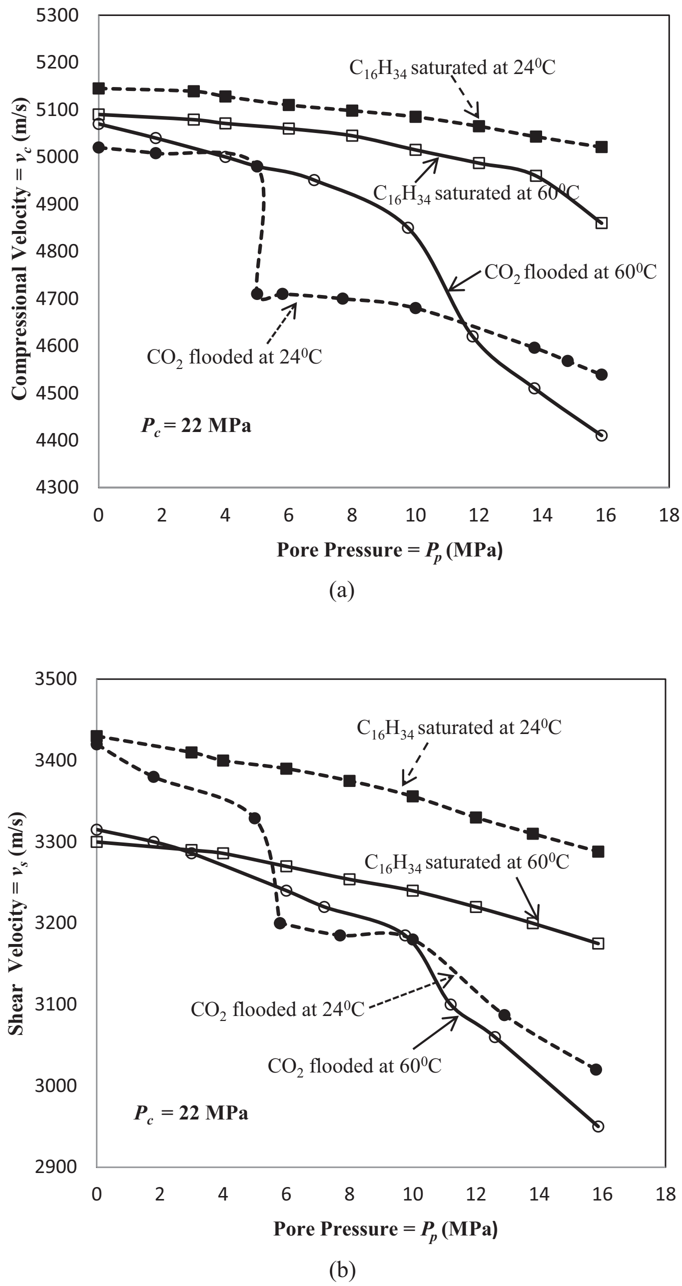

Fig. 6. (a) v_c in $C_{16}H_{34}$ saturated and CO_2 flooded N1 core plug vs. P_p. (b) v_s in $C_{16}H_{34}$ saturated and CO_2 flooded N1 core plug vs. P_p.

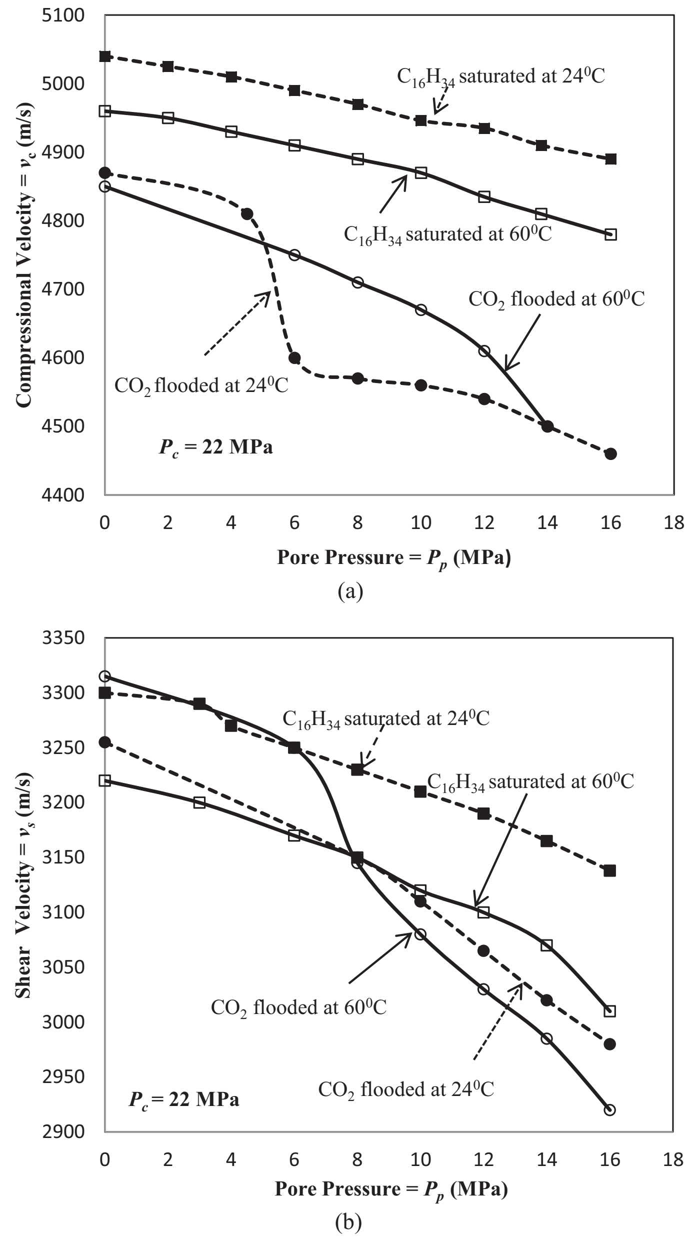

Fig. 7. (a) v_c in $C_{16}H_{34}$ saturated and CO_2 flooded N2 core plug vs. P_p. (b) v_s in $C_{16}H_{34}$ saturated and CO_2 flooded N2 core plug vs. P_p.

and b) was similar to that of N4 (Fig. 9a and b). The CO_2 flooding also decreased v_c. The v_c in LWP sand saturated with $C_{16}H_{34}$ are very sensitive to P_p changes (Fig. 11). CO_2 flooding decreased v_c dramatically at P_e of 20 MPa, i.e., zero P_p. This effect is larger in lower P_e. We were unable to measure v_s in LWP sand pack but believe that CO_2 would have very little effect on it.

3.1. *Comparing the velocities v_c and v_s with Gassmann's equation*

To extract crude oil from underground oil and gas reservoirs, we need a procedure to model fluid effects on rock velocity and density. Numerous techniques have been developed. However, Gassmann's equation was by far the most widely used relation to calculate v_c and v_s changes during hydrocarbon saturation and CO_2 flooding. The importance of this grows as v_c and v_s data are increasingly used for reservoir monitoring. Injecting CO_2 was shown to have large effects on decreasing the v_c in core plugs saturated with hydrocarbon ($C_{16}H_{34}$).

v_c and v_s in a homogeneous and isotropic elastic material are defined as:

$$v_c = \sqrt{\frac{K + \left(\frac{4}{3}\right)G}{\rho}} \tag{1}$$

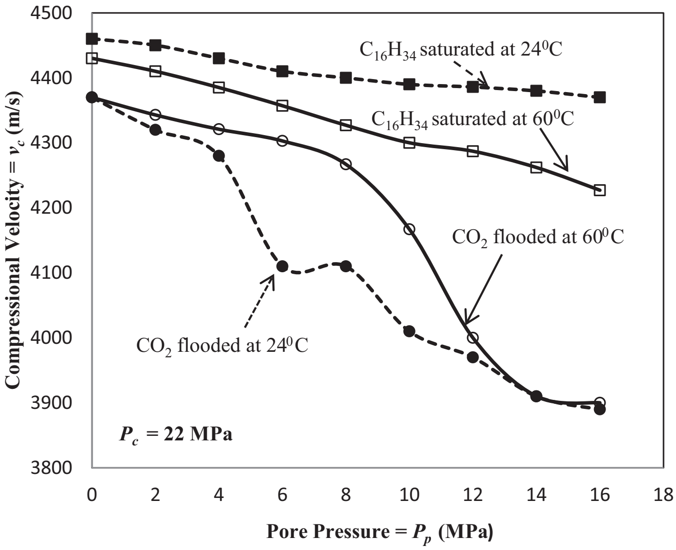

(a)

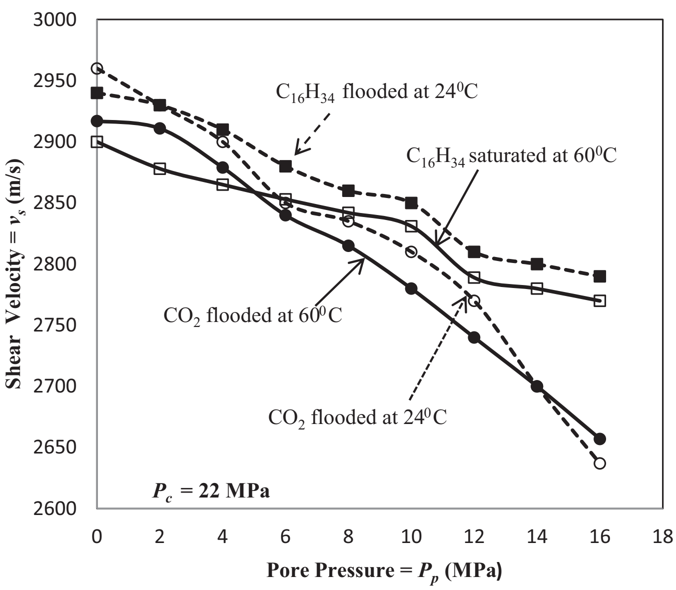

(b)

Fig. 8. (a) v_c in $C_{16}H_{34}$ saturated and CO_2 flooded N3 core plug vs. P_p. (b) v_s in $C_{16}H_{34}$ saturated and CO_2 flooded N3 core plug vs. P_p.

$$v_s = \sqrt{\frac{G}{\rho}} \tag{2}$$

where

K = bulk modulus
G = shear modulus
ρ = density of the material, kg/m^3

The Gassmann [43,44] equation relates the bulk modulus of the saturated rock to the properties of the rock and the pore fluid,

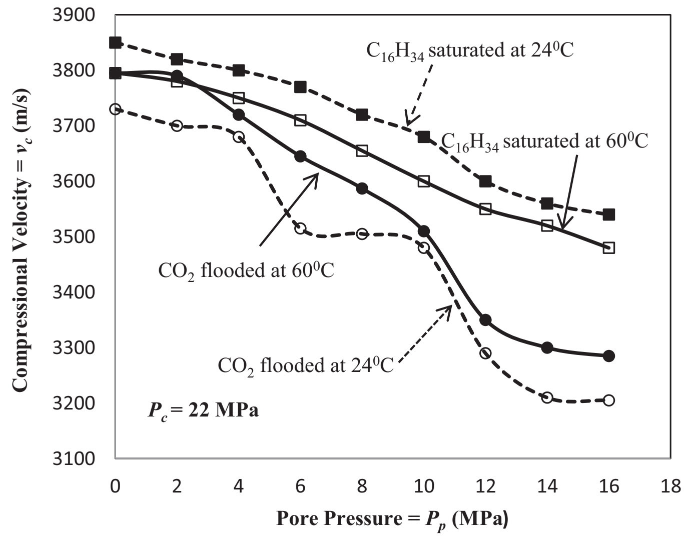

(a)

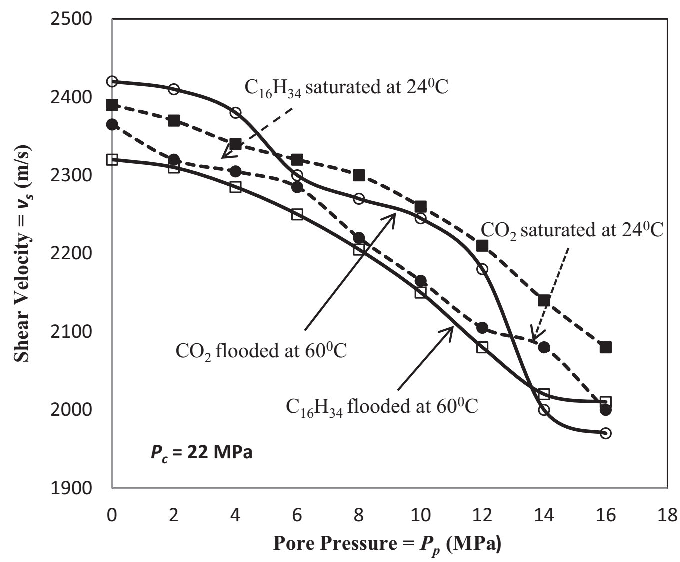

(b)

Fig. 9. (a) v_c in $C_{16}H_{34}$ saturated and CO_2 flooded N4 core plug vs. P_p. (b) v_s in $C_{16}H_{34}$ saturated and CO_2 flooded N4 core plug vs. P_p.

$$K = K_d + \frac{\left(1 - \frac{K_d}{K_s}\right)^2}{\frac{\varphi}{K_f} + \frac{(-\varphi)}{K_s} - \frac{K_d}{K_s}} \tag{3}$$

where

K_d = bulk modulus of dry porous media
K_s = bulk modulus of solid frame of the porous media
K_f = bulk modulus of solid frame of pore fluid
φ = porosity of the porous media, %

From the above Eqs. (1), (2) and (3), it can be seen that the velocity is related inherently to the viscosity (μ) of the fluid. The increase of μ can increase the porous media modulus and

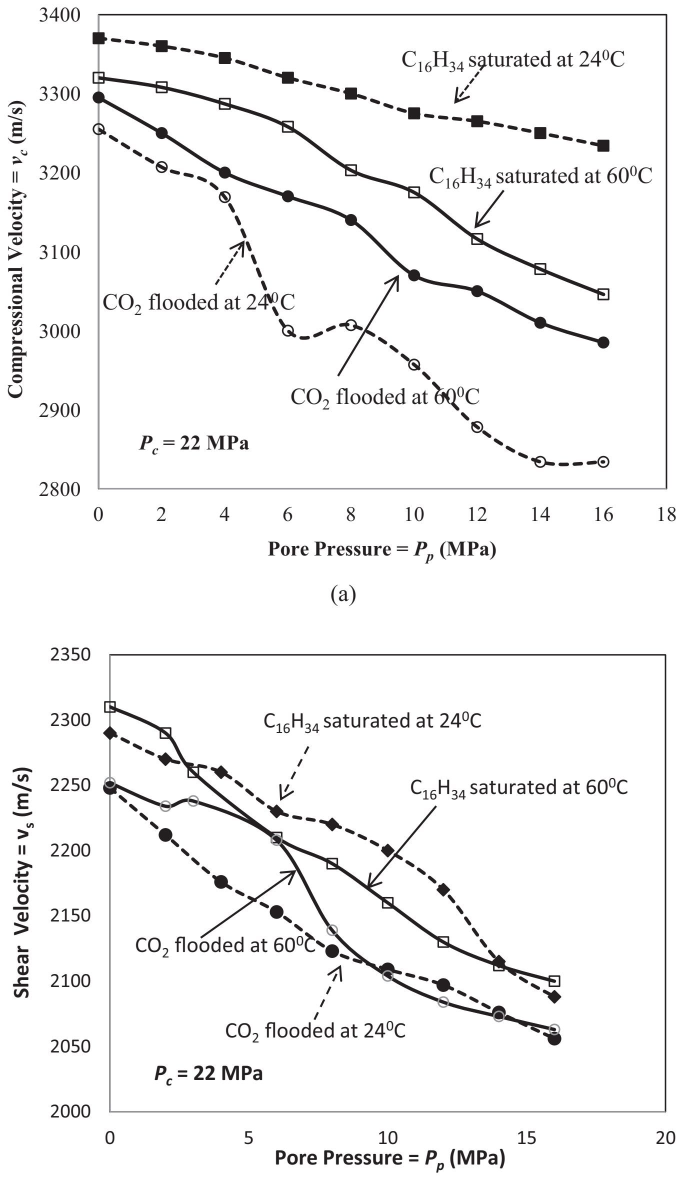

(a)

(b)

Fig. 10. (a) v_c in $C_{16}H_{34}$ saturated and CO_2 flooded N5 core plug vs. P_p. (b) v_s in $C_{16}H_{34}$ saturated and CO_2 flooded N5 core plug vs. P_p.

the velocity. The µ of $C_{16}H_{34}$ is greater than CO_2. So replacing $C_{16}H_{34}$ with CO_2 will decrease the µ of pore fluid, which will lead to the decrease of the velocity, as shown by the experimental results (Figs. 6–13). The relationship between the rock velocity and pore fluid µ can also be explained by Biot's theory qualitatively. The higher the µ of the fluid the stronger will be the coupling effect between the fluid and the rock skeleton of the porous media. This is equal to increasing the total rock rigidness and furthermore the velocity. Gassmann's equations [43] calculated the seismic response of CO_2 bearing rocks [45–50]. An attempt was made to compare the experimental v_c and v_s with the prediction by Gassmann's equation to confirm the experimental results. The experimental results show very close similarity to the results obtained by using Gassmann's equation (Figs. 12 and 13).

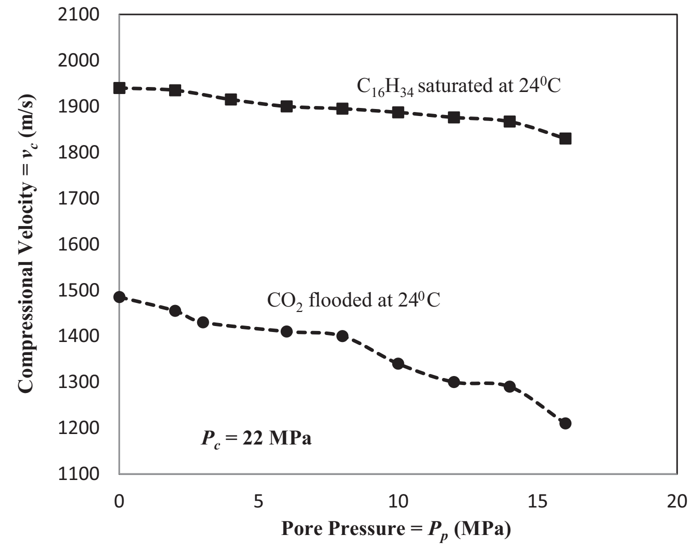

Fig. 11. v_c in $C_{16}H_{34}$ saturated and CO_2 flooded LWP sand pack vs. P_p.

3.2. Saturation and porosity

Equations (1) and (3) show that v_c in $C_{16}H_{34}$ saturated core plug depends on the properties of both the porous media and pore fluid. v_c of CO_2 flooded core plug was usually close to dry rock because the bulk modulus (incompressibility) of gas was usually very low [27]. While the bulk modulus of liquid is often comparable to dry rock, liquid saturation in core plug can increase v_c despite the increase in overall 'ρ' of the rock. When the core sample is partially saturated by $C_{16}H_{34}$, the bulk of the rock was about the same as that of dry rock, but the overall ρ was higher, so v_c can be even lower than dry or CO_2 flooded

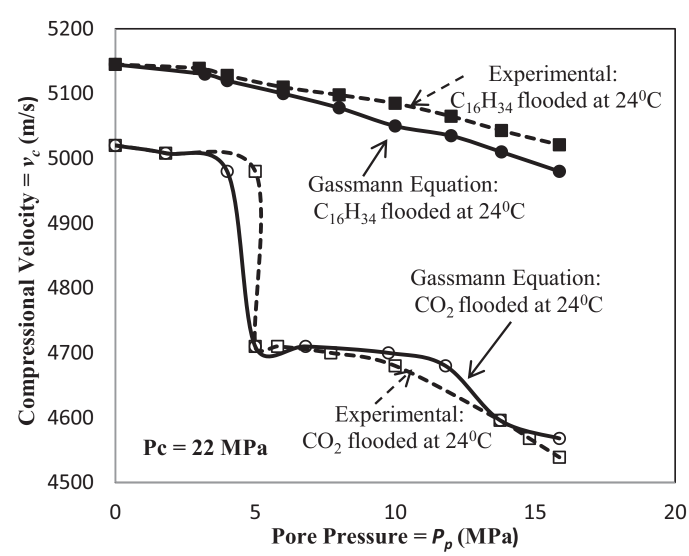

Fig. 12. Theoretically calculated v_c by Gassmann's equation and compared with experimental calculation v_c in N1 core plug flooded with CO_2 and saturated with $C_{16}H_{34}$ as a function of P_p.

Table 2
Results of the experiments on v_c and v_s from Figs. 6–10.

Figure no.	Core Plug	Porosity (%)	v_s or v_c	$[v_{(24°C)} - v_{(60°C)}][v_{(24°C)} - v_{(60°C)}]$ for $C_{16}H_{34}$ at P_p = 16 MPa	$[v_{(24°C)} - v_{(60°C)}][v_{(24°C)} - v_{(60°C)}]$ for $C_{16}H_{34}$ at P_p = 1 MPa	$[v_{(24°C)} - v_{(60°C)}][v_{(24°C)} - v_{(60°C)}]$ for CO_2 at P_p = 16 MPa	$[v_{(24°C)} - v_{(60°C)}][v_{(24°C)} - v_{(60°C)}]$ for CO_2 at P_p = 1 MPa
(1)	(2)	(3)	(4)	(5)	(6)	(7)	(8)
6(a)	N1	9.7	v_c	161	55	129	−50
6(b)			v_s	113	130	70	105
7(a)	N2	12.8	v_c	110	80	0	20
7(b)			v_s	128	80	60	−45
8(a)	N3	18.6	v_c	143	30	0	0
8(b)			v_s	20	40	−20	43
9(a)	N4	21.3	v_c	60	55	80	65
9(b)			v_s	70	70	30	−55
10(a)	N5	25.8	v_c	189	50	151	40
10(b)			v_s	37	58	25	38

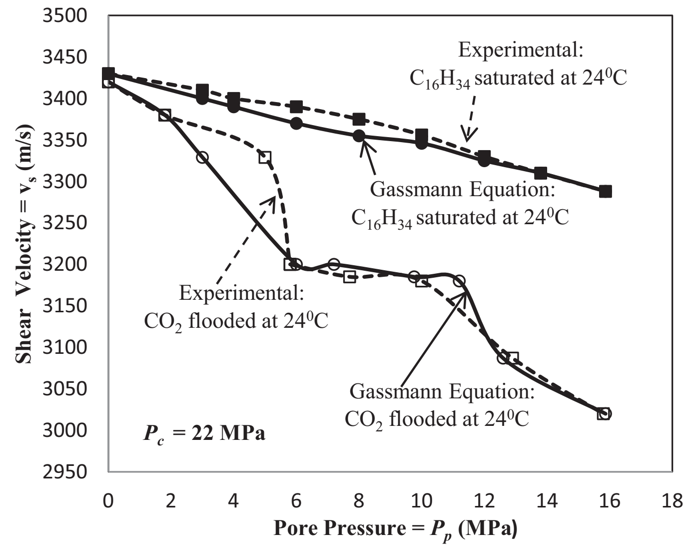

Fig. 13. Theoretically calculated v_s by Gassmann's equation and compared with experimental calculation v_s in N1 core plug flooded with CO_2 and saturated with $C_{16}H_{34}$ as a function of P_p.

cores (Eq. 1). v_c was dependent on the shear moduli and ρ (Eq. 2).

In low φ and high crack content core plugs like N1, N2 and N3 in Table 1, the liquid in the partially saturated cores usually occupies the cracks and thin pores, while the gas, i.e., CO_2, occupies the larger pores. This pattern of flow distribution usually causes the bulk moduli of the rock to be higher. The ρ increase caused by partial liquid saturation was less in low porosity cores. These combined effects in turn yield higher v_c (Eq. 1) which was the case of v_c in CO_2 flooded N1 (Fig. 6a), N2 (Fig. 7a), N3 (Fig. 8a) and N4 (Fig. 9a) below 5 MPa.

The phase transition of the injected CO_2 affected both v_c and v_s in the low φ N1 (Fig. 6b), N2 (Fig. 7b), and N3 (Fig. 8b). When injected CO_2 was in the liquid phase, its ρ is very high (1256.74 kg/m^3) even higher than $C_{16}H_{34}$ (793 kg/m^3), but its bulk modulus is still low. The higher ρ of liquid CO_2 in the core plugs were responsible for the low v_c and v_s in the flooded rock at P_p higher than 6 MPa. Above the critical temperature (31°C) of CO_2 density increases smoothly with pressure and the v_c and v_s also change smoothly with P_p as in Figs. 6–9 and Eqs. (1) and (2).

The v_s in the CO_2 flooded core plugs were lower than those in $C_{16}H_{34}$ saturated core at higher P_p but higher at lower P_p (Figs. 6b–9b) because of the effect of ρ, μ and P_p. At low P_p, higher v_s were caused by the low CO_2 ρ. At higher P_p, higher v_s in $C_{16}H_{34}$ saturated core plug are caused by the higher μ and lower ρ of the $C_{16}H_{34}$ in the core pores. During CO_2 injection the hydrocarbon bearing core was partially saturated with CO_2 with compressibility close to air. Therefore, the effect of CO_2 injection on the v_c should be close to that of P_p saturation, which depends on the φ of the cores [51,52].

The effect of CO_2 flooding on v_c change in % at different P_P at fixed temperature of 24°C and P_c of 22 MPa was plotted in Fig. 14. In core plugs increasing φ decreases CO_2 effect on v_c

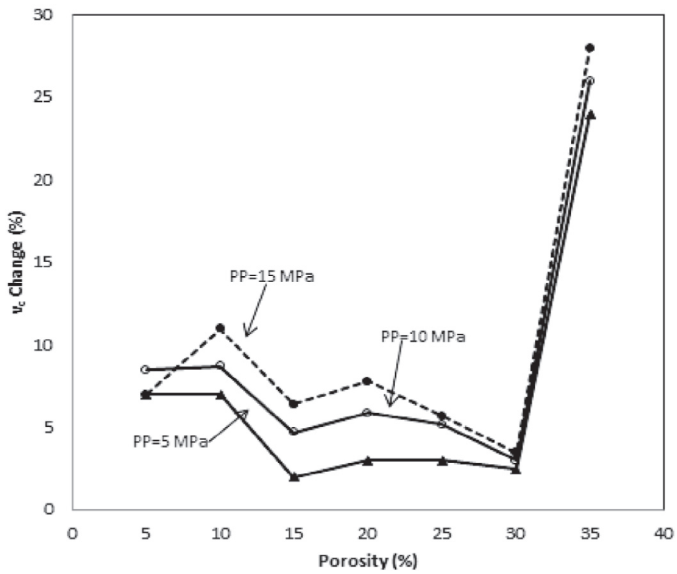

Fig. 14. Effect of CO_2 flooding on the v_c in $C_{16}H_{34}$ saturated core plug vs. porosity at different P_p.

[53]. In low φ core plugs as in Table 3, CO_2 caused a decrease in v_c up to 310 as in the case of N1 or 7.6%, while high φ core plugs like N5, the decrease is only 117 or 4.9%. In LWP sand pack, CO_2 decreased v_c by up to 70 or 31.8% even though the φ was as high as 47%.

According to Gassmann's equation (3), as the φ increases the bulk modulus (K) does not dramatically decrease very rapidly. The difference between the v_c in dry (in our case plugs saturated by CO_2 at 60 °C) and fluid saturated plugs will decrease as in Table 3, the difference between the v_c in dry and $C_{16}H_{34}$ saturated plugs at 24 °C and 60 °C or CO_2 flooded plugs at 24 °C will decrease owing to increased ρ and fluid content of the saturated plugs. Low φ plugs full liquid saturation greatly increases K but does not increase the ρ much, which in turn increases v_c markedly [54]. But for high φ plugs because the K of the pore fluid is usually much lower than that of the rock frame, liquid saturation has a smaller effect on the increase of K, but has a larger effect on the bulk ρ of the rock, which will not increase v_p as per Eq. (1). Other factors like cracks in rock, pore shapes and pore fluid properties contribute to liquid saturation which effects the v_c. The cracks in rocks and high μ of the pore fluid also increase the G of the rock. Therefore they increase both v_c and v_s (Eqs. 1 and 2) [25].

The unconsolidated LWP sand exhibited low v_c (Fig. 11) compared with the consolidated plugs (Figs. 6–10). Liquid saturation in LWP greatly increases its K and hence v_c (Eq. 1). Although liquid saturation also increases ρ, the increase in K plays a dominant role in unconsolidated sand [50].

3.3. Effect of CO_2 flooding by CO_2 and $C_{16}H_{34}$ saturation

The effects of CO_2 flooding and $C_{16}H_{34}$ saturation on the v_c at 24°C are shown in Table 3. The effect of $C_{16}H_{34}$ saturation on v_c was about the same as that of CO_2 flooding but with opposite signs in all the core plugs measured. After the core was CO_2 flooded, it becomes partially hydrocarbon saturated. Besides the φ and crack concentration of the core, the difference between the v_c in fully and partially $C_{16}H_{34}$ saturated may also depend on the degree of partial saturation. The effect of CO_2 injection depends on the amount of $C_{16}H_{34}$ displaced from the core plug. In the experiments, it was estimated that about 50–60% of the $C_{16}H_{34}$ in place were displaced.

3.4. Temperature effect

The effects of temperature in v_c and v_s in both CO_2 flooded and $C_{16}H_{34}$ saturated core plugs were discussed [25,48]. As seen in Figs. 5–13 increasing temperature in core plugs decreases the wave velocities, depending on φ, cracks in rocks and clay content of the core plugs. The decrease in the velocities is believed to be caused by softening of the rock frame and grains and an increase in φ resulting from different thermal expansion of the grains and cement [48,55,56]. The v_c usually have larger decrease in $C_{16}H_{34}$ saturated core plugs than in CO_2 flooded core plugs (Figs. 6a, 7a, 8a and 9a). Beyond the critical temperature CO_2 (31 °C) is in the vapour phase. At 24 °C (below critical temperature) a pronounced effect of CO_2 phase transition on the velocities in low porosity core plugs exists. This effect vanishes at temperatures higher than critical temperature of CO_2. Therefore, temperature will affect the CO_2 flooding effect on v_c in reservoir rock especially in the P_p range of 5–10 MPa. The ρ of CO_2 effect with temperature may play a dominant role especially in the P_p range of 5–10 MPa.

Table 3
Effect of CO_2 flooding and $C_{16}H_{34}$ saturation on v_c at 24 °C.

Sl. No.	Core plug	φ (%)	P_e = 5 MPa				P_e = 10 MPa				P_e = 15 MPa			
			Flooding by CO_2		Saturation by $C_{16}H_{34}$		Flooding by CO_2		Saturation by $C_{16}H_{34}$		Flooding by CO_2		Saturation by $C_{16}H_{34}$	
(1)	(2)	(3)	(4)	(5)	(6)	(7)	(8)	(9)	(10)	(11)	(12)	(13)	(14)	(15)
			Δv	−%	Δv	+%	Δv	−%	Δv	+%	Δv	−%	Δv	+%
1	N1	9.67	310	7.6	32	9.4	340	7.5	60	7.6	481	7.8	124	7.1
2	N2	12.8	60	8.0	40	11.7	310	8.6	90	9.6	365	7.9	180	8.9
3	N3	18.6	250	11.2	48	8.6	360	8.3	70	6.8	462	–	85	6.5
4	N4	21.3	145	8.2	70	11.8	285	4.8	170	9.4	267	3.5	285	7.5
5	N5	25.8	117	4.9	45	–	225	5.2	95	6.7	280	4.3	115	5.2
6	LWP sand	47	70	31.8	35	–	145	31.2	53	–	190	29.6	71	–

3.5. Pressure effect

The effect of P_c at constant P_p is to close the thin cracks and pores and make better contact between the grains and cement in the rock. Both v_c and v_s increase as P_c increases. The degree of increase in the velocities will depend on the cracks, φ, pore structure, geometry, mineral composition of the rock, pore fluid properties and interaction between the rock and fluid [57]. In contrast to P_c, P_p tends to keep cracks and pore open, hence it has opposite effect on velocities. In CO_2 bearing rocks, increasing P_p increases CO_2 density which in turn greatly decreases the velocities.

3.6. Porosity effect

In Fig. 15a and b it was observed that as the ?? increased in the core samples there was a decrease in v_c and v_s for both $C_{16}H_{34}$ and CO_2 at a constant P_e of 22 MPa. Through the literature reviews we can see that the v_c and v_s of core samples decrease with the increase of φ the influence of shale content on the velocities is much more complicated; for the sandstone with good consolidation, the increase of clay content will lead to the decrease of velocities, but it will cause a slight increase in the velocities for the sandstone with weak consolidation [58–62].

3.7. Compressional and shear velocity by Gassmann's equation

The Gassmann equation (3) was used to calculate low frequency wave velocity in cores saturated with hydrocarbon ($C_{16}H_{34}$) and flooded by CO_2. The calculated results are plotted and were compared with the experimental results in Figs. 12 and 13 for N1 core plugs. The calculated v_c and v_s in N1 saturated with $C_{16}O_{34}$ were only slightly lower than those of the experimental results (Figs. 12 and 13). The calculated v_c and v_s in N1 flooded with CO_2 were almost the same with only slight variations when compared with the experimental results (Figs. 12 and 13). Furthermore, both the experimental and theoretical results calculated by Gassmann equation (3) reveal that this CO_2 effect may be seismically detectable. Therefore seismic methods may be used in monitoring CO_2 flooding process.

3.8. Seismic monitoring

The capability of using seismic methods to monitor EOR process depends solely on the velocity and/or amplitude changes of the seismic waves caused by the process. The amplitude changes are usually difficult to measure in the laboratory or field, while velocity changes can be usually detected with high accuracy.

The experimental results in Fig. 14 show that v_c decreased as the core was flooded by CO_2 specially in high P_p. The decreased v_c and v_s in core plugs of reservoir rocks during CO_2 flooding cause travel time delay of seismic waves. Therefore high frequency and resolution seismic methods can be used in monitoring CO_2 flooding process in the reservoir for EOR [63–65]. According to the experimental results the injected CO_2 forms low velocity zones (Figs. 6–11). The largest effect of CO_2 on the v_c occurs at P_p higher than 6 MPa. In the field the injected pressure of CO_2 into the reservoir is usually around 7 MPa or higher. Velocities in hydrocarbon saturated fully or partially rocks have proved to be frequency dependent [66,67]. The relative changes of velocities caused by CO_2 flooding will help in monitoring CO_2 flood front.

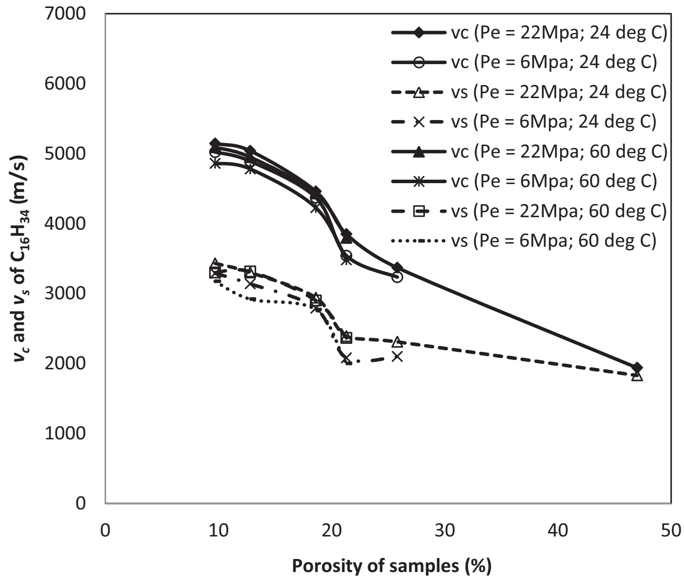

(a)

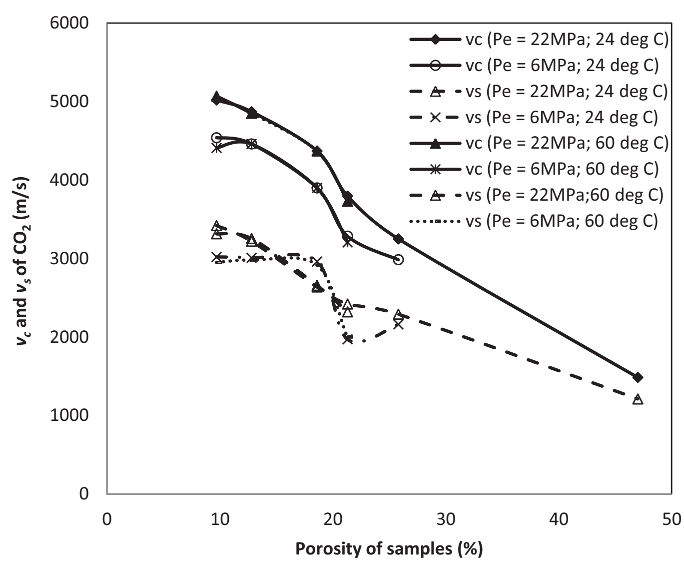

(b)

Fig. 15. (a) v_c and v_s in $C_{16}H_{34}$ saturated core samples and LWP sand pack vs. porosity. (b) v_c and v_s in CO_2 flooded core samples and LWP sand pack vs. porosity.

4. Conclusion

It was found that CO_2 flooding has a significant effect on v_c in sandstones saturated with $C_{16}H_{34}$. CO_2 flooding decreased v_c from 4 to 12% in well consolidated sandstone and by more than 30% in unconsolidated sand. Large decrease in v_c in rocks depends on P_p, temperature, porosity (φ) and other factors.

Increasing P_p at constant P_c not only keeps the pores and cracks open, but also nullifies some of the P_c effect and increases CO_2 density. Higher P_p cause larger decreases in both v_c and shear velocity v_s.

In consolidated sandstones, increasing φ tends to decrease the CO_2 effect. The decrease effect in high φ rock is caused by the increased fluid content and overall ρ of the rocks. In unconsolidated sand, the flooding effect is very large, even though the φ of the sand is high, because the K of the sand is low. The decrease in v_c caused by CO_2 flooding makes it possible to use seismic methods in mapping CO_2 zones, tracking CO_2 front movement and monitoring flooding processes in reservoirs subjected to CO_2 flooding.

Acknowledgements

We would like to acknowledge the Indo-US Project F. No. 194-1/2009(IC) dated 20.2.15 titled "Foam-assisted CO_2 Flooding for the depleted Reservoirs of Upper Assam Basin and in Candidate Reservoirs in Louisiana" of 21st Century Knowledge Initiative Program under University Grants Commission. Thanks are also extended to all individuals associated with the project.

References

[1] S.B. Gogoi, K.D. Gogoi, Evaluation of lignin based surfactants for enhanced oil recovery of Naharkatiya Porous Media, Indian Chem. Eng. J. 50 (2008) 47–55.
[2] S.B. Gogoi, Revisiting Naharkatiya core sample for enhanced oil recovery, Indian J. Pet. Geol. 18 (2009) 51–61.
[3] S.B. Gogoi, Adsorption of non-petroleum base surfactant on reservoir rock, Curr. Sci. 97 (2009) 1059–1063.
[4] S.B. Gogoi, Characterization of vesicle for enhanced oil recovery, Indian J. Chem. Technol. 17 (2010) 282–290.
[5] S.B. Gogoi, Adsorption of a lignin-based surfactant on Naharkatiya Porous Media, Indian Chem. Eng. J. 52 (2010) 1–11.
[6] S.B. Gogoi, Adsorption–desorption of surfactant for enhanced oil recovery, Transp. Porous Media 90 (2011) 589–604.
[7] S.B. Gogoi, B.M. Das, Use of an effluent for enhanced oil recovery, Indian J. Chem. Technol. 19 (2012) 366–370.
[8] B.M. Das, S.B. Gogoi, Relating IFT with oil recovery with special reference to Bhogpara Porous Media of Upper Assam Basin, J. Pet. Eng. Technol. 5 (2015) 1–8.
[9] K. Hazarika, S.B. Gogoi, Comparative study of an enhanced oil recovery process with various chemicals for Naharkatiya oil field, Int. J. Appl. Sci. Biotechnol. 2 (2014) 432–436.
[10] D.W. Lynch, T.R. Lewis, W.J. Moorman, J.R. Burg, D.H. Groth, A. Khan, et al., Carcinogenic and toxicologic effects of inhaled ethylene oxide and propylene oxide in F 344 rats, Toxicol. Appl. Pharmacol. 76 (1984) 69–84.
[11] P.L. Desbene, B. Desmazières, V. Even, J.J. Basselier, L. Minssieux, Analysis of non-ionic surfactants used intertiary oil recovery, optimisation of stationary phase in normal phase partition chromatography, Chromatographia 24 (1987) 857–861.
[12] J. Patel, S.B. Gogoi, V. Rangarajan, P. Somasundaran, R. Sen, Recent developments in microbial enhanced oil recovery, Renew. Sustain. Energy Rev. 52 (2015) 1539–1558.
[13] R. Rico-Martínez, T.W. Snell, T.L. Shearer, Synergistic toxicity of Macondo crude oil and dispersant Corexit 9500 A® to the Brachionusplicatilis species complex (Rotifera), Environ. Pollut. 173 (2013) 5–10.
[14] C. Mulligan, R. Yong, B. Gibbs, Surfactant-enhanced remediation of contaminated soil: a review, Eng. Geol. 60 (2001) 371–380.
[15] S.B. Gogoi, Carbon-dioxide for EOR in Upper Assam Basin, in: M.Z. Hou, H. Xie, P. Were (Eds.), Clean Energy Systems in the Subsurface: Production, Storage and Conversion, Springer Series in Geomechanics and Geoengineering, Germany, 2013, pp. 157–169.
[16] E. Tzimas, A. Georgakaki, C.G. Cortes, S.D. Peteves, Enhanced Oil Recovery Using Carbon Dioxide in the European Energy System, European Commission, Directorate General Joint Research Centre, Petten, The Netherlands, 2015.
[17] J. Moortgat, Viscous and gravitational fingering in multiphase compositional and compressible flow, Adv. Water Resour. 89 (2016) 53–66.
[18] L. Stephen Melzer, Carbon dioxide enhanced oil recovery (CO_2 EOR): factors involved in adding carbon capture, utilization and storage (CCUS) to enhanced oil recovery CO_2. February 2012. http://neori.org/Melzer_CO2EOR_CCUS_Feb2012.pdf.
[19] W.E. Johnson, R.M. Macfarlane, J.N. Breston, D.C. Neil, Laboratory experiments with carbonated water and liquid carbon dioxide as oil recovery agents, Producers Mon. 17 (1952) 18–22.
[20] J.W. Martin, Additional oil production through flooding with carbonated water, Producers Mon. 15 (1951) 18–22.
[21] L.W. Holm, Carbon dioxide solvent flooding for increased oil recovery processes, Petrol. Trans. 216 (1959) 225–231.
[22] A.V. Kane, Performance review of a large-scale CO_2-WAG enhanced recovery project, SACROC Unit – Kelly-Snyder field, J. Pet. Technol. 31 (1979) 217–231.
[23] M. Sen, R. Zhang, High resolution seismic inversion for CO_2 mapping from time-lapse seismic data, in: Proceedings of International Conference of CO_2 Injection for EOR, NGRI Hyderabad, 26–28 November 2012.
[24] R. Hope, D. Ireson, J. Meyer, W. Tittle, M. Willis, Seismic integration to reduce risk, Oilfield Rev. 10 (1998) 2–15.
[25] Z. Wang, A.M. Nur, Effects of CO_2 flooding on wave velocities in rocks with hydrocarbons, SPE Reserv. Eng. 4 (1989) 429–436.
[26] P. Schutjens, W. Heidug, Pore volume compressibility and its application as a petrophysical parameter, Presented in the 9th Biennial International Conference & Exposition in Petroleum Geophysics, Hyderabad, 2012.
[27] A.R. Gregory, Fluid saturation effects on dynamic elastic properties of sedimentary rocks, Geophysics 41 (1976) 895–921.
[28] G. Simmons, Ultrasonics in geology, Proc. Inst. Electr. Electron. Eng. 53 (1965) 1337–1345.
[29] M. Ganesapillai, P. Simha, The rationale for alternative fertilization: equilibrium isotherm, kinetics and mass transfer analysis for urea-nitrogen adsorption from cow urine, Resour. Efficient Technol. 1 (2015) 90–97.
[30] M. Ganesapillai, P. Simha, K. Desai, Y. Sharma, T. Ahmed, Simultaneous resource recovery and ammonia volatilization minimization in animal husbandry and agriculture, Resour. Efficient Technol. 2 (2016) 1–10.
[31] P. Simha, K. Desai, A. Yadav, D. Pinjari, A.B. Pandit, On the behaviour, mechanistic modelling and interaction of biochar and crop fertilizers in aqueous solutions, Resour. Efficient Technol. 2 (2016) 133–142.
[32] H. Ecke, Fluids, pressures and frequencies in porous rocks (M.Phil. thesis), Colorado School of Mines, 2004.
[33] M.A. Kassab, A. Weller, Study on P-wave and S-wave velocity in dry and wet sandstones of Tushka region, Egypt, Egypt. J. Pet. 24 (2015) 1–11.
[34] Z. Wang, A. Nur, Wave velocities in hydrocarbon-saturated rocks: experimental results, Geophysics 55 (1990) 723–733.
[35] Z. Wang, A. Nur, Elastic wave velocities in porous media: a theoretical recipe, in: Z. Wang, A. Nur (Eds.), Seismic and Acoustic Velocities in Reservoir Rocks, 1992, 2, pp. 1–35.
[36] J. Hilsenrath, C.W. Beckett, Tables of Thermal Properties of Gases, National Bureau of Standards, Whitefish, MT, 2013.
[37] N.B. Vargaftik, Tables on the Thermophysical Properties of Liquids and Gases, second ed., Halsted Press, Division of John Wiley & Sons, Inc., New York, 1975.
[38] M.S. King, Wave velocities in rocks as a function of changes in overburden pressure and pore fluid saturants, Geophysics 31 (1966) 50–73.
[39] (a) M.A. Biot, Theory of propagation of elastic waves in a fluid saturated porous solid, J. Acoust. Soc. Am. 28 (1956) 168–191; (b) A. El-Suleiman,

N.B. Anosike, P. Pilidis, A preliminary assessment of the initial compression power requirement in CO2 pipeline "Carbon Capture and Storage (CCS) technologies", Technologies 4 (2016) 15.

[40] Z. Wang, M.L. Batze, A.M. Nur, Effect of different pore fluids on seismic velocities in rocks, Can. J. Explor. Geophys. 26 (1990) 104–112.

[41] E.S. Abreu, Theoretical modeling and empirical research applied to the connection between the petrophysical properties and Elastic in carbonate rocks (Master Thesis), UNICAMP, Sao Paulo, Brazil, 2010, 129.

[42] F. Gassmann, Elastic waves through a packing of spheres, Geophysics 16 (1951) 673–685.

[43] D. Makarynska, B. Gurevich, J. Behura, M. Batzle, Fluid substitution in rocks saturated with viscoelastic fluids, Geophysics 75 (2010) 15–122.

[44] J.J. Mckenna, B. Gurevich, M. Urosevic, B.J. Evans, Rock physics-application to geological storage of CO_2, APPEA J. 43 (2003) 567–576.

[45] X. Lei, Z. Xueb, Ultrasonic velocity and attenuation during CO_2 injection into water-saturated porous sandstone: measurements using difference seismic tomography, Phys. Earth Planet. Inter. 176 (2009) 224–234.

[46] Z. Wang, Fundamentals of seismic rock physics, Geophysics 66 (2001) 398–412.

[47] Z. Wang, Dynamic versus static properties of reservoir rocks, in: Z. Wang, A. Nur (Eds.), Seismic and Acoustic Velocities in Reservoir Rocks, Society of Exploration Geophysicists, Tulsa, 2000, 19, pp. 531–539.

[48] S.H. Kazemeini, C. Juhlin, S. Fomel, Monitoring CO_2 response on surface seismic data; a rock physics and seismic modeling feasibility study at the CO_2 sequestration site, Ketzin, Germany, J. Appl. Geophys. 71 (2010) 109–124.

[49] J. Carcione, S. Picotti, D. Gei, G. Rossi, Physics and seismic modeling for monitoring CO_2 storage, Pure Appl. Geophys. 163 (2006) 175–207.

[50] Z. Liu, J. Zhao, An experimental study of velocity-saturation relationships in volcanic rocks, Pet. Eng. J. 8 (2015) 142–152.

[51] B.L. Alemu, E. Aker, M. Soldal, O. Johnsen, O. Aagaard, A CO_2 flooding experiment of brine saturated sandstone in a CT-scanner, Energy Procedia 4 (2011) 4379–4386.

[52] L.A. Binyam, A. Eyvind, S. Magnus, J. Øistein, A. Per, Influence of CO_2 on rock physics properties in typical reservoir rock: a CO_2 flooding experiment of brine saturated sandstone in a CT-scanner, Energy Procedia 4 (2011) 4379–4386.

[53] R. Nolen-Hoeksema, Modulus–porosity relations, Gassmann's equations, and the low-frequency elastic-wave response to fluids, Geophysics 65 (2000) 1355–1363.

[54] H. Kern, Elastic wave velocity in crustal and mantle rocks at high pressure and temperature: the role of high-low quartz transition and dehydration reactions, Phys. Earth Planet. Inter. 29 (1982) 12–23.

[55] H.K. Chen, F.T. Wu, D.M. Jenkins, J. Mechie, S.W. Roecker, C.Y. Wang, et al., Seismic evidence for the α-β quartz transition beneath Taiwan from Vp/Vs tomography, Geophys. Res. Lett. 39 (2012) 1–6.

[56] A. Hassanzadegan, G. Blöcher, H. Milsch, L. Urpi, G. Zimmermann, The effects of temperature and pressure on the porosity evolution of Flechtinger sandstone, Rock Mech. Rock Eng. 47 (2014) 421–434.

[57] B.Z. Wang, Seismic rock physics and its applied research, Ph.D. Thesis, Chengdu University of Science and Technology, Chengdu, 2008 (in Chinese).

[58] G. Shi, D.Q. Yang, The regression analysis study on velocity and porosity and clay content of rocks, Acta Sci. Nat. Univ. Pekinesis 37 (2001) 379–384.

[59] T. Klimentos, The effects of porosity-permeability-clay content on the velocity of compressional waves, Geophysics 56 (1991) 1930–1939.

[60] J. Dvorkin, G. Mavko, A. Nur, Squirt flow in fully saturated rocks, Geophysics 60 (1995) 97–107.

[61] X. Huang, L. Meister, R. Workman, Improving production history matching using time-lapse seismic data, Leading Edge 17 (1998) 1430–1433.

[62] H. Rogno, K. Duffaut, A.K. Furre, L.B. Kvamme, Calibration of time lapse seismic to well and production data – examples from the Statfjord Field, in: 61st EAGE Conference and Exhibition: Reservoir Monitoring and Management, Finland, EAGE, 1999.

[63] P.W. Gabriels, N.A. Horvei, J.K. Koster, A. Onstein, A. Geo, R. Staples, Time lapse seismic monitoring of the Draugen Field, SEG Technical Program Expanded Abstracts (1999) 2035–2037.

[64] D.E. Lumley, M. Bee, S. Jenkins, Z. Wang, 4-D seismic monitoring of an active steamflood, in: 65th Ann. Internat. Mtg: Soc. of Expl. Geophys., (1995) 203–206.

[65] D. Han, Effect of porosity and clay content on acoustic properties of sandstones and unconsolidated sediments (Doctoral dissertation), October 1986. https://srb.stanford.edu/sites/default/files/srb_028_oct86_han.pdf.

[66] Z. Wang, Wave velocities in hydrocarbon and hydrocarbon saturated rocks; with applications to EOR monitoring (Doctoral dissertation), April 1988. https://srb.stanford.edu/sites/default/files/srb_034_apr88_wang.pdf.

[67] M. Ganesapillai, A. Singh, Separation processes and technologies as the mainstay in chemical, biochemical, petroleum and environmental engineering: a special issue, Resour. Efficient Technol. 2 (2016) S1–S2.